INTERNATIONAL JOURNAL OF CONSERVATION SCIENCE
ISSN: 2067-533X Volume 12, Issue 3, July-September 2021: 1077-1090 www.ijcs.ro

UTILIZATION OF THERMALLY ACTIVATED WATER-WASHED KAOLIN PARTICLES TOWARDS MINERAL RESOURCES CONSERVATION

Shahrul Azwan SHAKRANI[1,*], Afizah AYOB[1],
Mohd Asri AB RAHIM[1], Salina ALIAS[2]

[1] Faculty of Civil Engineering Technology, Universiti Malaysia Perlis (UniMAP), Kompleks Pusat Pengajian Jejawi 3, 02600 Arau, Perlis, Malaysia
[2] Faculty of Civil Engineering, Universiti Teknologi MARA (UiTM), Cawangan Pulau Pinang, 13500 Permatang Pauh, Pulau Pinang, Malaysia

Abstract

Sustainable utilization of kaolin has brought benefits to the conservation of mineral resources and economic alternatives to construction materials that rely heavily on commercial Portland cement. Industrially produced water-washed kaolin particles can be thermally activated to meet requirements as supplementary cementitious materials, depending on temperature and duration of calcination. In this study, samples were calcined at temperatures of 600-800°C and durations of 3-4 hours to determine the optimum conditions for the development of metakaolin as supplementary cementitious materials. Using techniques such as PSA, BET, SEM/EDX, FTIR and XRD, water-washed kaolin particles were analyzed and significant differences were observed between the properties of each sample. At 800°C and 3-4 hours, samples were successfully transformed from kaolinite to metakaolinite. This change increased the distribution of multimodal particle sizes, decreased BET surface area, and loss of hexagonal kaolinite morphology. Besides, the weight and atomic percentage of O, Al, Si and K decreased, but C increased. Al-O-H peaks also disappeared, while Si-O peaks were transformed into a single broad peak of amorphous silica. In addition, the kaolinite reflections vanished, but quartz remained. However, complete dehydroxylation of kaolinite was successfully achieved due to increased disorder and defective behavior of samples which were believed to facilitate further transformation into metakaolinite.

Keywords*: Kaolin; Calcination; Clay; Kaolinite; Metakaolin; X Ray Diffraction; Scanning Electron Microscopy; Sustainable Utilization*

Introduction

Kaolin is a phyllosilicates or layer silicates mineral that originates from the occurrence of chemical weathering in the sedimentary rocks. These minerals are usually made up of aluminosilicate minerals such as pure kaolinite, illite, montmorillonite, halloysite, nacrite and dickite, as well as mineral impurities such as quartz, smectite, feldspar and mica. The production of kaolin can be found in more than 50 countries with an estimated annual output of over 16 million metric tonnes [1]. Kaolin can be considered as one of the primary sources of materials in the modern industry and has been widely used in many fields of application, such as the arts, sculptures, architectural, historical monuments, building materials, ceramics,

* Corresponding author: shahrulazwan.shakrani@gmail.com

refractory materials, fillers, polymers, rubbers, agricultural, chemicals, particles packing, coatings, paints, cosmetics, paper processing, pharmaceuticals and water treatments [2, 3].

Effective utilization of kaolin can be achieved through the exploitation of mineral deposits at fully capacity involving the extraction and processing of precious components. It has also added benefits to the conservation of mineral resources and economically viable alternatives, especially for construction materials that are largely dependent on commercially well-known Portland cement [4, 5]. The sustainable utilization of mineral resources is related to the balance between exploitation and conservation concerns. This is truly important to efficiently utilize the mineral resources for the economical gains, while at the same time reducing waste, land disturbances and environmental impacts. Therefore, the mineral resources exploitation must also take into account the nature of reserves, utilization and extraction practices, environmental conditions and post-mining conditions.

These kaolin minerals can be further processed and utilized to meet the desired level of brightness, color, grade, gloss, impurity, opacity, residue, particle size, product life, viscosity and weight. Usually, the procedure is often referred to as water-washed, which involves a thorough cleaning of the kaolin particles. This complex technique involves processes such as blunging, slurrying, degritting, separating, centrifuging, settling, filtering, brightening, drying, powdering and packing [6].

For the purpose of construction materials, the water-washed kaolin particles can be thermally activated for the application as supplementary cementitious materials. This thermal activation, or also known as calcination, is a thermal treatment of solids at very high temperatures in the absence of air or oxygen with the purpose of removing undesirable compositions at the desired level. During thermal activation, the interlayer, hydrate and absorbed water were removed from the surface of the kaolinite particle, and the crystalline lattice structures were completely or partially broken [7]. The transition phase of highly disordered, amorphous and pozzolanic material led to the formation of metakolinite [8]. In the meantime, prolonged exposure to temperature caused recrystallization activities, and the formation of spinel or mullite, resulting in a loss of pozzolanicity ability [8, 9]. Complete dehydroxylation of kaolinite mineral and the development of metakaolinite during transformation in the form of a chemical reaction is described in Equation 1 as follows [10, 11]:

$$Al_2O_3 \cdot 2SiO_2 \cdot 2H_2O\ (\text{Kaolinite}) \rightarrow Al_2O_3 \cdot 2SiO_2\ (\text{Metakaolinite}) + 2H_2O\ (\text{Water}) \uparrow \quad (1)$$

Calcination period and temperatures are very important and have an influence on the mineralogical changes of the kaolin particles. Kaolin minerals calcined at temperatures between 600 to 800°C have shown pozzolanic reactivity and can be used to accelerate the cement hydration at about 5 to 10% replacement rate from the total mass of ordinary Portland cement in concrete mixtures [12, 13]. During calcination, kaolinite dehydroxylation produces an amorphous phase known as metakaolinite. This metakaolinite produces reactive silica and alumina that can react with calcium hydroxide through pozzolanic activity, depending on the degree of dehydroxylation and the accommodation or surface available for reaction [14].

There are many advantages of metakaolin as a supplementary cementitious material, such as helping to reduce CO_2 emissions and energy consumption due to no additional clinkering process involved in the production of cement for cleaner and more sustainable materials [15]. Besides, metakaolin particles help provide a nucleating agent to promote hydration due to high reactivity, encourage higher levels of silica and alumina particularly in comparison to other supplementary cementitious materials, good micro-filling effects, and enhance the mechanical and durability properties of materials [16]. In the process of assessing new materials as supplementary cementitious materials, the relevant characteristics must be carried out in order to determine their performance aspects. Supplementary cementitious materials are commonly evaluated for physical and chemical properties, such as particle size

distribution, specific surface area, morphology, chemical composition, phase identification and mineralogy, which may have an impact on pozzolanic activities and the interaction between cement hydration and water demand [17-19].

In the present study, water-washed kaolin particles were thermally activated at varying temperatures and duration to determine the optimal conditions of the kaolin particles undergoing the calcination process for the development of metakaolin as supplementary cementitious material. Thermal activation of this type of kaolin particles is currently not well understood and the background properties of this material need to be explored in depth for future potential applications. In order to fulfill this purpose, the water-washed kaolin particles were analyzed using instrumental techniques such as Zetasizer Particle Size Analyzer (PSA), Brunauer-Emmett-Teller Surface Area (BET), Scanning Electron Microscopy with Energy Dispersive X-Ray (SEM/EDX), Fourier Transform Infrared Spectroscopy (FTIR) and X-Ray Diffraction (XRD). Significant differences were observed between the properties of water-washed kaolin particles subjected to thermally activation at different temperatures and duration.

Experimental part

Materials

Water-washed kaolin particles were purchased from Kaolin (Malaysia) Sdn Bhd and marketed under the KM65 label. These kaolin particles were thermally activated at calcination temperatures of 600-800°C, period of 3-4 hours and heating rate of 10°C/min using Carbolite GPC1200 general purpose industrial chamber furnace (Carbolite Gero Limited, UK). The calcination conditions used in the study are briefly described in Table 1.

Table 1. Calcination conditions

Sample	Description	Temperature (°C)	Period (hours)	Heating Rate (°C/min)
K	Control	0	0	0
MK 600-3	Thermally Activated	600	3	10
MK 600-4	Thermally Activated	600	4	10
MK 700-3	Thermally Activated	700	3	10
MK 700-4	Thermally Activated	700	4	10
MK 800-3	Thermally Activated	800	3	10
MK 800-4	Thermally Activated	800	4	10

Methods

The particle size of samples with refractive index of 1.57 was determined by Zetasizer Nano ZS Particle Size Analyzer (Malvern Instruments, UK) using dynamic light scattering at backscatter angle of 173°, under temperature of 25°C, with viscosity of 0.8872cP and refractive index of 1.33. Brunauer-Emmett-Teller (BET) surface area was examined using Micromeritics TriStar 3000 Surface Area and Pore Size Analyzer (Micromeritics Instrument Corp, USA) at -195.8°C with nitrogen adsorption after 3 hours of outgassing at 200°C. Sample morphology was captured using Scanning Electron Microscopy (SEM) JEOL JMS-6460LA (JEOL Ltd., Japan) with magnification up to 10,000× and 10kV voltage. This instrument was also designed with Energy Dispersive X-Ray Spectroscopy (EDX) JED-2300 AnalysisStation (JEOL Ltd., Japan) for elemental identification. The functional group was analyzed using Fourier Transform Infrared Spectroscopy (FTIR) Perkin Elmer Spectrum 65 (PerkinElmer Inc., USA) at 4cm^{-1} resolution with 100 scans ranging from 4000 to 450cm^{-1}. The mineralogy properties were detected at scanning speed of 0.02sec/step from 4° to 70° of 2θ using X-Ray Powder Diffraction (XRD) Bruker D2 Phaser Benchtop (Bruker, USA) operating with copper target of 30kV and 10mA, as well as wavelength of Kα1 = 1.5406Å and Kα2 = 1.54439Å.

Results and discussion

Particle Size Analysis (PSA)

Figure 1 demonstrates cumulative and average particle size distribution of water-washed kaolin particles subjected to thermal activation at different temperatures and duration.

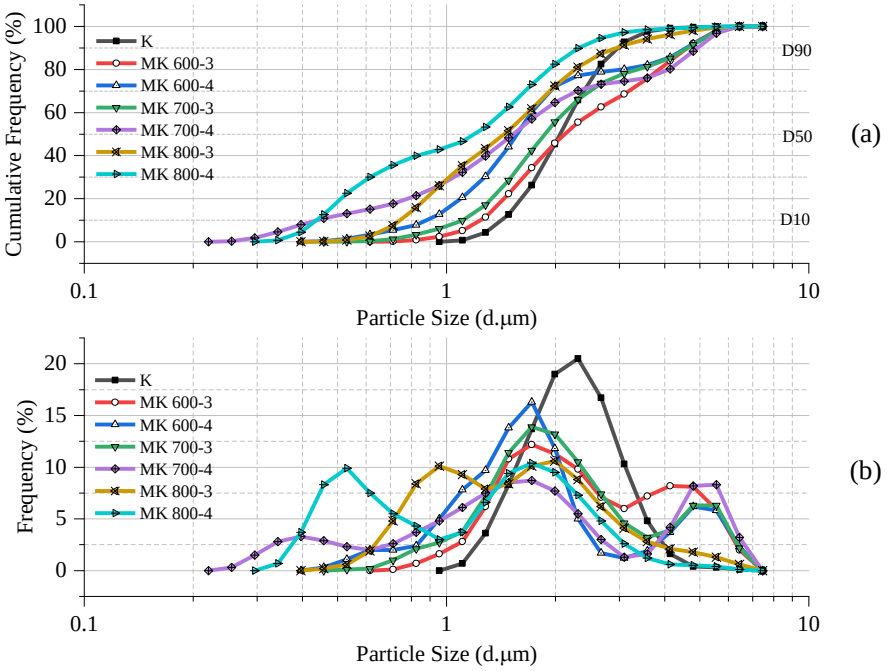

Fig. 1. Cumulative (a) and average (b) particle size distribution of water-washed kaolin particles subjected to thermal activation at different temperatures and duration

The cumulative distribution of the particle size indicated 100% of the water-washed kaolin particles passing 7.456µm sizing when subjected to thermal activation, which is similar to that found in the control sample. All effective sizes of D_{10}, D_{50}, and D_{90} in water-washed kaolin particles exposed to thermal activation were found to be smaller than the control sample, with the exception of D_{90} in the MK 600-3, MK 600-4, MK 700-3 and MK 700-4 samples, ranging between 0. 2202 and 7.456µm sizing. However, the average particle size of the water-washed kaolin particles increased when subjected to thermal activation compared to the control sample. This can be seen in average particle sizes: 4.168±0.8781, 4.295±0.3453, 4.327±1.348, 4.415±1.577, 4.445±0.8628, 4.609±2.254 and 4.635±1.841µm by increasing calcination temperatures and duration. Thermal activation has led to an increase in the average particle size and aggregation with the greater formation of coarser particles at the expense of finer particles by increasing calcination temperatures and duration. This is due to the agglomeration produced by sintering and recrystallization that caused an increase in the coarser particle's region [20,21]. In addition, the distribution of water-washed kaolin particles transformed from unimodal to bimodal and trimodal distributions containing submicron and micron particles by increasing calcination temperatures and duration. This is caused by the formation of aggregate structures through partial fusion of kaolin particles during thermal activation, which has also affected the distribution of particles size [22]. This was confirmed by the classification of the mid-range polydisperse type of particles broadness obtained by the polydispersity index values ranging from 0.359±0.109 to 0.526±0.254.

Brunauer-Emmett-Teller (BET) Surface Area

The adsorption isotherm of water-washed kaolin particles subjected to thermal activation at different temperatures and duration is described in figure 2.

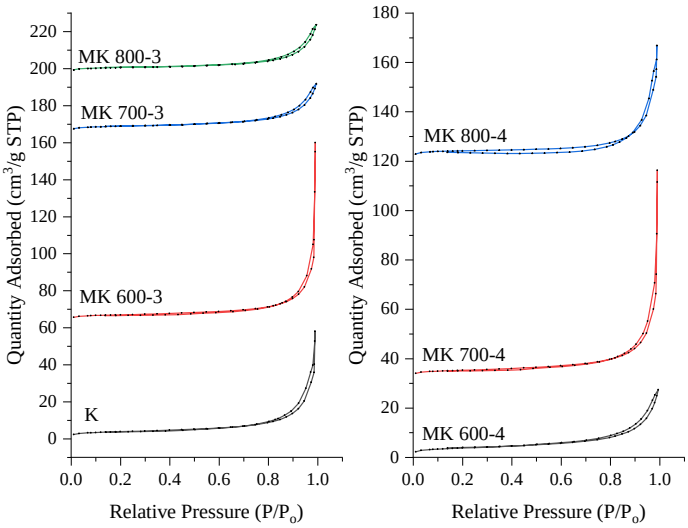

Fig. 2. Adsorption isotherm of water-washed kaolin particles subjected to thermal activation at different temperatures and duration

According to the IUPAC classification [23], all samples of water-washed kaolin particles exhibited H3-type of hysteresis loops. The absence of plateau at high P/P° in these samples indicated partial mesopore filling that can never be regarded as type IV isotherms. This type of isotherm showed typical characteristics of type II isotherms for both adsorption and desorption branches until the critical P/P° was achieved. The monolayer-multilayer adsorption of water-washed kaolin particles samples in the present study revealed the common behavior of non-rigid aggregates of plate-like particles, such as clay minerals. Under type II, all these isotherms displayed two different kinds of isotherm shapes. Samples K, MK 600-3, MK 700-4 and MK 800-4 were grouped in a similar shape, whereas samples MK 600-4, MK 700-3 and MK 800-3 were grouped in a different shape. Meanwhile, the BET specific surface area of the water-washed kaolin particles subjected to thermal activation at different temperatures and duration is shown in table 2. The BET specific surface area of the water-washed kaolin particles decreased to 13.514, 13.302, 13.065, 12.968, 12.330 and 12.307m^2/g by increasing the calcination temperatures and duration compared to the control sample at 13.603m^2/g. This is caused by kaolin particles clustering into more coarsening particles during thermal activation, which has also been observed in the present particle size analysis. As a result, particle agglomeration led to a reduction in the BET specific surface area of the water-washed kaolin particles. Such observations are consistent with the findings previously reported suggesting that an increase in particle size may reduce the BET specific surface area of kaolin [9, 24].

Table 2. BET specific surface area of water-washed kaolin particles subjected to thermal activation at different temperatures and duration

Sample	K	MK 600-3	MK 600-4	MK 700-3	MK 700-4	MK 800-3	MK 800-4
Surface Area (m^2/g)	13.603	13.514	13.302	13.065	12.968	12.330	12.307

Scanning Electron Microscopy (SEM)

Figure 3 presents the SEM images of water-washed kaolin particles subjected to thermal activation at different temperatures and duration.

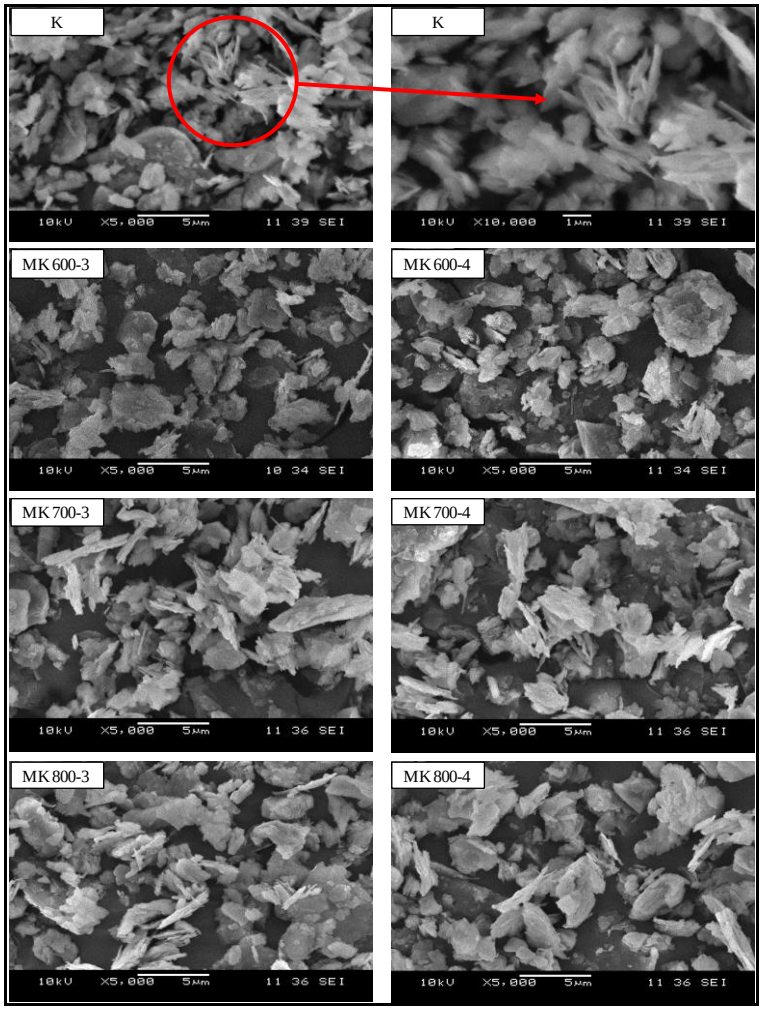

Fig. 3. SEM of water-washed kaolin particles subjected to thermal activation at different temperatures and duration

Water-washed kaolin particles for the control sample displayed the typical behavior of the kaolinite microstructure, which can be evidenced by the pseudo-hexagonal shape of the crystals and the layered structure of the booklet morphology. These kaolin particles are made up of very few perfect hexagonal kaolinite crystals that indicates the behavior of the high-defect and disorder structure. The flaky texture of small, flat and flake crystals originated from the lamellar structure of kaolinite was also observed in this sample. However, the individual flakes showed a sign of anhedral crystal structure due to the existence of a pseudo-hexagonal of irregular shapes with small particles of a broken edge. This disorder structure was caused by the presence of contaminants and poorly crystalline conditions during their formation, which were responsible for inhomogeneity in the distribution of particle sizes [13, 25]. This was in good agreement with the particle size analysis which confirmed the bimodal distribution of the

particle size that contributed to heterogeneity. In addition, the procedures involved in the water-washing process during the production of kaolin particles have also amounted to this microstructure. As water-washed kaolin particles underwent thermal activation, the morphology of kaolin particles witnessed of kaolinite crystals with hexagonal outlines and several lobed flakes at temperatures of 600°C. Although kaolin particles have achieved complete dehydroxylation, the calcination temperature of 600°C does not alter the basic hexagonal platelet shape of kaolinite particles. Besides, the lamellar texture of the kaolin particles appeared to be denser and extended by increasing the calcination duration from 3 to 4 hours. Calcination temperatures at 700°C and 800°C also did not alter the general platy shape of kaolinite, but their particle edges became more rounded and began to lose their hexagonal shape. The agglomeration of platelets in irregular stacks became more apparent, which was also demonstrated by previous findings in [7, 26]. At this stage, kaolinite flakes become more deformed and locally compacted into clusters with uneven and multiple splitting of thicker flake packets witnessed by increasing the calcination duration from 3 to 4 hours. It can therefore be established that thermally activated of water-washed kaolin particles have shown no substantial difference from control sample, but their books are more open and exhibited horizontal shifts or rotations between layers as the lamellar texture appears to widen by increasing calcination temperatures and duration.

Energy Dispersive X-Ray Spectroscopy (EDX)

The EDX of water-washed kaolin particles subjected to thermal activation at different temperatures and duration is shown in figure 4.

Five elements, including C, O, Al, Si and K, were found at the EDX peaks of the water-washed kaolin particles. The availability of Al, Si and O in water-washed kaolin particles implies that these elements are prominent components of clay minerals such as kaolin along with C and K impurities. By increasing calcination temperatures and duration, the weight and atomic percentage of C was found to be higher in water-washed kaolin particles subjected to thermal activation compared to the control sample. The weight percentages of C for MK 600-3, MK 600-4, MK 700-3, MK 700-4, MK 800-3 and MK 800-4 samples were found at 39.05, 43.88, 40.03, 46.51, 42.88 and 44.91%, while the atomic percentages of C for MK 600-3, MK 600-4, MK 700-3, MK 700-4, MK 800-3 and MK 800-4 samples were found at 49.52, 54.02, 51.07, 56.99, 53.62 and 55.63%, compared to the control samples of K at 31.16% and 41.28%, respectively.

It was suggested that the increased in the C element was due to the carbonation reaction involved in the calcination process. However, the increase in calcination temperatures and duration caused the weight and atomic percentage of the elements O, Al, Si and K to decrease in the thermally activated water-washed kaolin particles compared to the control sample. Weight percentages of O, Al, Si and K elements were found at 42.29, 9.14, 8.88 and 0.63% for MK 600-3, 41.11, 7.72, 6.80 and 0.50% for MK 600-4, 39.02, 10.24, 10.07 and 0.64% for MK 700-3, 37.71, 7.56, 7.51 and 0.72% for MK 700-4, 38.93, 8.93, 8.66 and 0.60% for MK 800-3, and 37.65, 8.65, 8.29 and 0.50% for MK 800-4, compared to the K sample at 45.73, 11.39, 10.91 and 0.80%, respectively. In the meantime, the atomic percentages of O, Al, Si and K elements were detected at 40.26, 5.16, 4.82 and 0.25% for MK 600-3, 37.99, 4.23, 3.58 and 0.19% for MK 600-4, 37.37, 5.82, 5.49 and 0.25% for MK 700-3, 34.69, 4.12, 3.93 and 0.27% for MK 700-4, 36.54, 4.97, 4.63 and 0.23% for MK 800-3 and 35.02, 4.77, 4.39 and 0.19% for MK 800-4, compared to the K sample at 45.49, 6.72, 6.18 and 0.33%, respectively.

This is due to structural and chemical changes in kaolinite that are transformed into metakolinite stage during the thermal activation. In addition, the Si/Al ratio of water-washed kaolin particles was found to be higher in the weight percentage relative to the atomic percentage ranged from 0.88 to 0.99 which is lower than the pure kaolinite Si/Al ratio at 1. At a lower Si/Al ratio, kaolinite is becoming more persistent, but the crystallization of kaolinite is

more favored at higher temperatures and helps to gradually increase the amorphous hump in the formation of metakaolinite [27, 28].

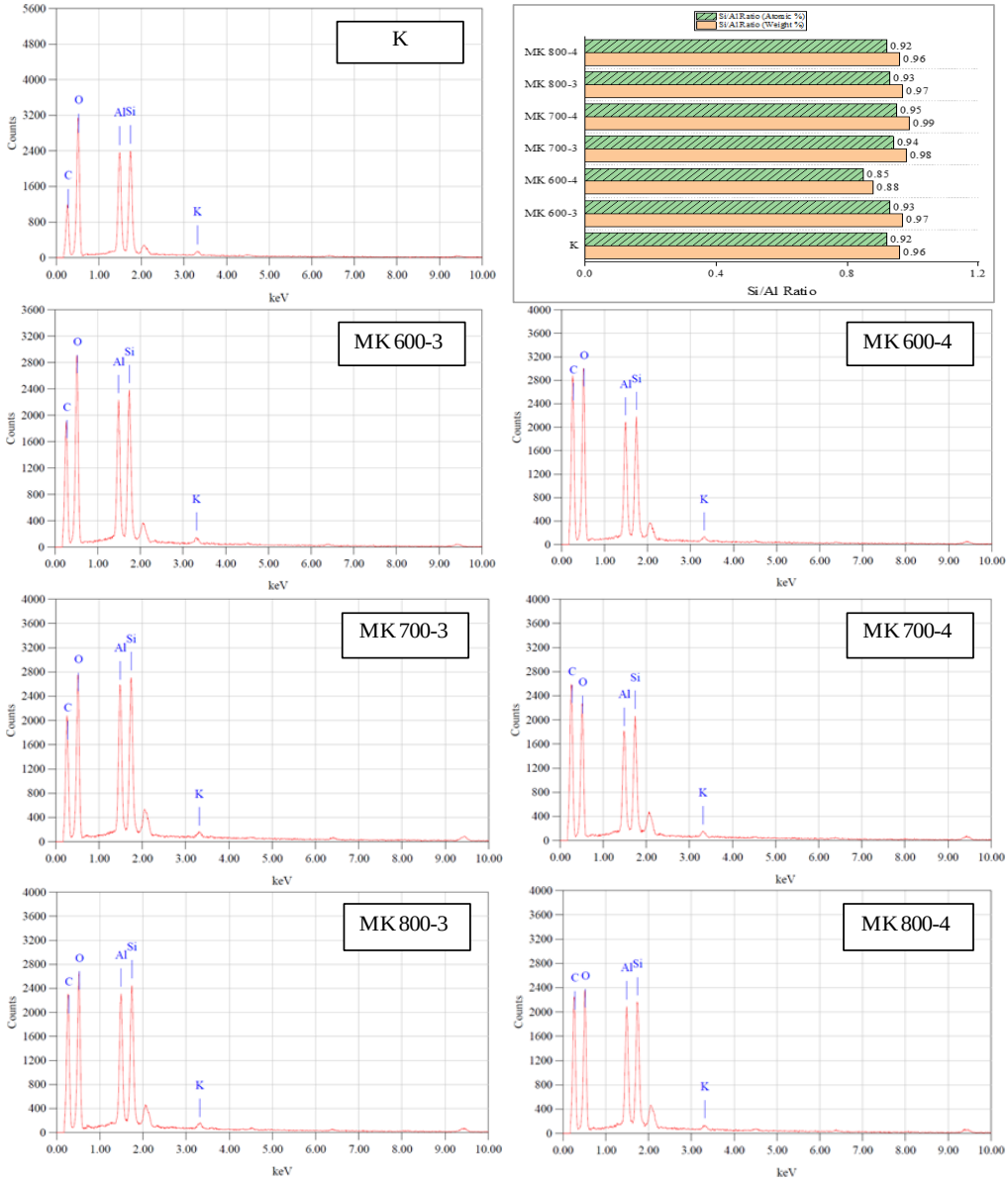

Fig. 4. EDX of water-washed kaolin particles subjected to thermal activation at different temperatures and duration.

Fourier Transform Infrared Spectroscopy (FTIR)

Figure 5 displays the FTIR of water-washed kaolin particles subjected to thermal activation at different temperatures and duration.

The control sample of K indicated the typical behavior of kaolinite. The absorption band at 3697cm^{-1} was formed by Al-O-H stretching of inner-surface hydroxyls, while the peak at 3620cm^{-1} was designated to the Al-O-H stretching of inner hydroxyls. The infrared spectrum of the 3446 and 1635cm^{-1} bands was assigned to the H-O-H stretching and bending of absorbed

and coordinated water. Peak at 1115cm^{-1} suggested Si-O stretching out of plane vibration mode, while absorption bands at 1031 and 1007cm^{-1} were caused by Si-O stretching in plane vibration mode.

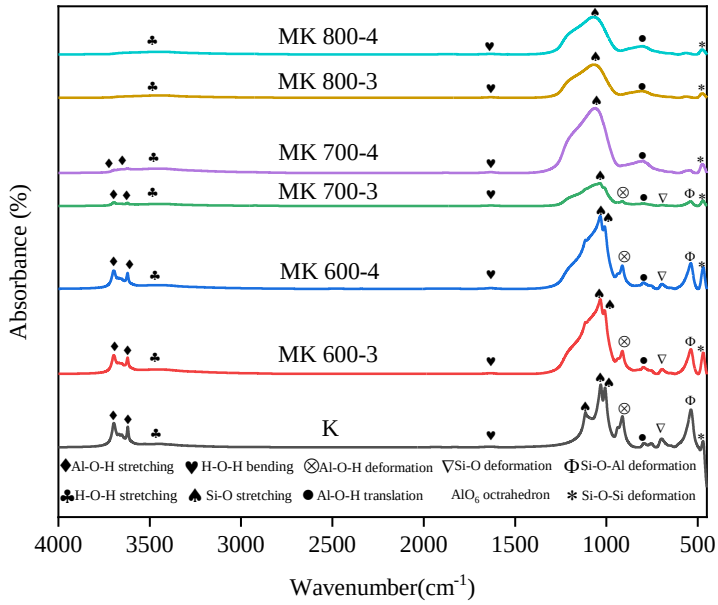

Fig. 5. FTIR of water-washed kaolin particles subjected to thermal activation at different temperatures and duration

The band at 913cm^{-1} was associated with the Al-O-H deformation of inner hydroxyls while the peak at 796cm^{-1} was related to the Al-O-H translation mode. The absorption band at 698cm^{-1} was assigned to the perpendicular deformation of the Si-O bond. Peak at 536cm^{-1} was due to Si-O-Al deformation mode, while the IR spectrum at 471cm^{-1} band was attributed to Si-O-Si deformation mode. The absorbance intensity of the infrared spectra of water-washed kaolin particles subjected to thermal activation at different temperatures and duration increased from the original sample due to modifications in thermal treatment of the kaolinite surfaces. Besides, the stretching and deformation vibrations of hydroxyls are in particular highly sensitive to changes in hydroxyl surfaces during calcination. This resulted in the opposite changes in the low and high frequency components of absorption bands of the structural O-H groups due to the manifestation of thermal expansion [29, 30]. The temperature of 600°C was not enough to break the crystalline structure of the kaolin particles. Although the IR spectra of the water-washed kaolin particles in the MK 600-3 and MK 600-4 samples decreased from the original sample, but there was not much difference between the absorption peaks of these samples. However, in the MK 600-3 and MK 600-4 samples, the peak at 1115cm^{-1} of Si-O stretching out of plane vibration in the control sample disappeared. At temperature of 700°C, the Si-O stretching in plane at 1011 cm^{-1} disappeared in the MK 700-3 and MK 700-4 samples. Al-O-H deformation of inner hydroxyls and Si-O-Al deformation still occurred at a peak of 913 and 539cm^{-1} in the MK 700-3 sample but vanished in the MK 700-4 sample. Meanwhile, Si-O stretching in plane at peak of 1035cm^{-1} still appeared in the sample of MK 700-3 but shifted at peak of 1071cm^{-1} due to broadening of Si-O stretching in MK 700-4 sample. New peak at 559cm^{-1} was observed in the MK 700-4 sample due to stretching of AlO_6 octrahedron indicating the formation of metakaolinite. However, the Al-O-H stretching of inner-surface hydroxyls at peaks of 3697 and 3694cm^{-1} and the Al-O-H stretching of inner hydroxyls at peaks 3622 and 3622cm^{-1} also showed evidence of incomplete dehydroxylation. At temperature of 800°C, All

Al-O-H stretching and deformation of inner-surface and inner hydroxyls disappeared in the MK 800-3 and MK 800-4 samples, suggesting complete dehydroxylation of kaolinite and conversion to metakaolinite. The O-H bands have vanished due to an increase in the kinetic energy of atoms during thermal activation [31]. The broadening of Si-O stretching bands at 1060 and 1072 cm^{-1} led to the transformation into a very strong and broad peak. The absence of Si-O stretching and deformation indicated the transition of Si-O vibrations from sharp shoulder peaks to a single broad peak indicating the characteristics of amorphous silica [32]. The loss of Al-O-Si deformation band entails significant structural changes in the local environment of the Al and Si atoms in the octahedral and tetrahedral sheets [33]. The presence of new absorption bands at 564 and 563 cm^{-1} due to stretching of AlO6 octrahedron results in dehydroxylation during calcination and kaolinite undergoes thermal transformation to amorphous metakaolinite.

X-Ray Powder Diffraction (XRD)

The XRD of water-washed kaolin particles subjected to thermal activation at different temperatures and duration is depicted in figure 6.

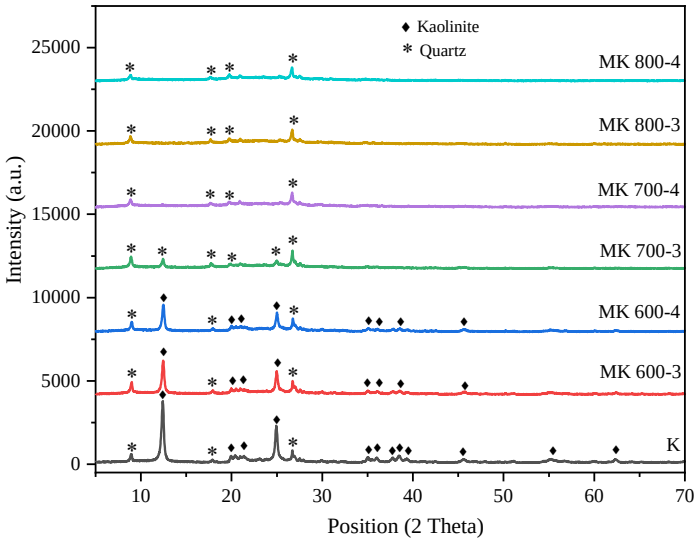

Fig. 6. XRD of water-washed kaolin particles subjected to thermal activation at different temperatures and duration

The XRD analysis of the water-washed kaolin particles in the control K sample was dominated by 99% of the kaolinite (Al_2 Si_2 O_9) reflections. Two predominant peaks of kaolinite were found in regions 001 and 002 near 12.43 and 24.89° of 2θ in the form of anorthic crystals with a *P* 1(1) space group. The remaining peaks contained quartz (Si_{24} O_{48}) which appeared in the form of hexagonal crystal in the *P* 6_2 (171) space group and were found in the region of 011 and 321 near 8.98 and 26.70° of 2θ. Low-intensity peaks near 20 and 22° of 2θ indicated the behavior of poorly ordered kaolinite which may contribute to the transformation of water-washed kaolin particles into highly relative metakaolinite during thermal activation. At temperature of 600°C, there was no significant change between thermally activated water-washed kaolin particles of MK 600-3 and MK 600-4 samples to the control sample. The kaolinite peaks still appeared but decreased from 99 to 97% due to a break in the kaolinite bonding layers. However, the reflections of kaolinite in the region of 001 and 002 near 12.47 and 24.97° of 2θ in the MK 600-3 sample were shifted to 12.51 and 25.00° of 2θ in the MK 600-4 sample. The quartz peaks of MK 600-3 and MK 600-4 samples increased from 1 to 3% but maintained the hexagonal shape and *P* 6_2 (171) space group of the original sample. In the region of 011 and 32, the prominent quartz peaks were slightly moved from 8.98 and 26.73 ° of

2θ in the MK 600-3 sample to 9.01 and 26.75° of 2θ in the MK 600-4 sample. However, the water-washed kaolin particles subjected to 600°C temperature in duration of 3 to 4 hours remained unchanged from the original sample, indicating by highly crystalline behavior and the absence of amorphous phase in the XRD patterns. At temperature of 700°C, kaolinite reflections vanished from the thermally activated water-washed kaolin particles of MK 700-3 and MK 700-4 samples due to significant loss in crystallinity during calcination. The x-ray diffraction was transformed from a highly crystalline phase to a semi-amorphous phase of crystal. Quartz remained in the MK 700-3 sample even though the modification and transformation of the crystal structures occurred during calcination. High reflections of quartz were observed near 8.91, 12.44, 17.69, 24.95 and 26.72° of 2θ in the region of 110, 200, 211, 020 and 101. Similarly, the MK 700-4 sample was also dominated by reflections of the hexagonal shape of quartz. Major peaks in the regions of 110, 220, 031, 100, 101 and 131 were detected at 8.88, 17.69, 19.72, 20.92, 26.67 and 27.47° of 2θ. At temperature of 800°C, complete calcination was achieved, without the presence of kaolinite reflections, and quartz remained unchanged, stable and no transformation occurred in the thermally activated water-washed kaolin particles of MK 800-3 and MK 800-4 samples. Major peaks of quartz were observed in the 110, 220, 002, 101 and 121 regions near 8.85, 17.66, 19.73, 26.72 and 27.50° of 2θ in the MK 800-3 sample, but were shifted to 8.86, 17.63, 19.73, 26.68 and 27.48° of 2θ in the MK 800-4. In addition, polymorphic forms of quartz, such as tridymite and crystobalite was not observed at calcination temperatures below 1000°C. Kaolinite peaks completely disappeared due to significant decreased in crystallinity, major loss of hydroxyl groups and breaking of the kaolinite layers bonds [9, 10, 30]. The absence of kaolinite peaks also implied the complete transformation of kaolinite into amorphous metakaolinite due to dehydroxylation of the kaolinite structure and can be observed by hump broadening or better known as amorphization [7, 33].

Conclusions

Water-washed kaolin particles were activated by thermal treatment at varying temperatures and duration in order to determine the optimum conditions for the development of metakaolin as supplementary cementitious material towards conservation of mineral resources. Using instrumental techniques such as PSA, BET, SEM, EDX, FTIR and XRD, the properties of thermally activated water-washed kaolin were evaluated and conclusions were drawn as follows. At an optimum temperature of 800°C and a duration of 3 to 4 hours, the water-washed kaolin particles were successfully transformed from kaolinite to metakaolinite state during thermal activation. The average particle size of thermally activated water-washed kaolin particles increased from the original sample together with the transition from unimodal into bimodal and trimodal distributions containing submicron and micron particles. As a result, the BET specific surface area of thermally activated water-washed kaolin particles decreased from the original sample. However, the general platy morphology of thermally activated water-washed kaolin particles remained unchanged from the original sample, but the edges of the particle were more rounded and lost their typical hexagonal shape.

In addition, the agglomeration of platelets in irregular stacks became more apparent, and their books became more open, showing horizontal shifts or rotation between layers as the lamellar structure began to expand. The weight and atomic percentage of the O, Al, Si and K elements decreased in both control and thermally activated water-washed kaolin particles, but the C element increased due to calcination. All Al-O-H stretching and deformation of inner-surface and inner hydroxyls disappeared in the thermally activated water-washed kaolin particles suggesting complete dehydroxylation of kaolinite and conversion to metakaolinite. Besides, Si-O stretching, deformation and vibrations transformed from sharp shoulder peaks to a single broad peak indicates the characteristics of amorphous silica. Kaolinite peaks

completely disappeared due to significant decreased in crystallinity, major loss of hydroxyl groups and breaking of the kaolinite layers bonds but quartz reflections remained unchanged and not affected. The absence of kaolinite peaks indicated the complete transformation of kaolinite from highly crystalline phase into amorphous metakaolinite due to dehydroxylation of the kaolinite structure. Based on these findings, the complete dehydroxylation of kaolinite was successfully attained due to increased disorder and defective behavior of the water-washed kaolin particles and believed to promote greater transformation into metakaolinite.

Acknowledgments

The first author is grateful for the financial support from the Ministry of Higher Education, Malaysia and Universiti Malaysia Perlis through the Skim Latihan Akademik Bumiputera (SLAB) scholarship during his PhD study. Special thanks to the technical staff at Universiti Malaysia Perlis and Universiti Teknologi MARA for their assistance and contribution during the PSA, BET, SEM, EDX, FTIR and XRD analysis.

References

[1] D. Prasetyoko, M. Santoso, I. Qoniah, W.L. Leaw, P.B. Firda, H. Nur, *A review on synthesis of kaolin-based zeolite and the effect of impurities*, **Journal of the Chinese Chemical Society**, **67**, 2020, pp. 911– 936.

[2] J. Ondruška, Š. Csáki, V. Trnovcová, I. Štubňa, F. Lukáč, J. Pokorný, L. Vozár, P. Dobroň, *Influence of mechanical activation on DC conductivity of kaolin*, **Applied Clay Science**, **154**, 2018, pp. 36-42.

[3] S.A. Shakrani, A. Ayob, M.A. Ab Rahim, S. Alias, *Stability of kaolin particles subjected to elevated temperatures using various dispersing agents*, **Journal of Physics: Conference Series**, **1529**, 2020, pp. 042099.

[4] K.P. Seong, *Sustainable mining of the clay resources in Peninsular Malaysia*, **Geological Society of Malaysia Bulletin**, **51**, 2005, pp. 1-5.

[5] W. Xu, X. Wen, J. Wei, P. Xu, B. Zhang, Q. Yu, H. Ma, *Feasibility of kaolin tailing sand to be as an environmentally friendly alternative to river sand in construction applications*, **Journal of Cleaner Production**, **205**, 2018, pp. 1114-1126.

[6] S.A. Shakrani, A. Ayob, M.A. Rahim, S. Alias, *Properties of pulverized kaolin particles via ball-to-powder weight ratios milling process: XRF and Zetasizer particle size analysis*, **IOP Conference Series: Earth and Environmental Science**, **476**, 2020, pp. 012070.

[7] B. Ilić, V. Radonjanin, M. Malešev, M. Zdujić, A. Mitrović, *Effects of mechanical and thermal activation on pozzolanic activity of kaolin containing mica*, **Applied Clay Science**, **123**, 2016, pp. 173-181.

[8] M. Said-Mansour, E.H. Kadri, S. Kenai, M. Ghrici, R. Bennaceur, *Influence of calcined kaolin on mortar properties*, **Construction and Building Materials**, **25**, 2011, pp. 2275-2282.

[9] A. Souri, F. Golestani-Fard, R. Naghizadeh, S. Veiseh, *An investigation on pozzolanic activity of Iranian kaolins obtained by thermal treatment*, **Applied Clay Science**, **103**, 2015, pp. 34-39.

[10] B.R. Ilić, A.A. Mitrović, L.R. Miličić, *Thermal treatment of kaolin clay to obtain metakaolin*, **Hemijska Industrija**, **64**, 2010, pp. 351-356.

[11] A. Shvarzman, K. Kovler, G.S. Grader, G.E. Shter, *The effect of dehydroxylation/amorphization degree on pozzolanic activity of kaolinite*, **Cement and Concrete Research**, **33**, 2003, pp. 405-416.

[12] H. Abdul Razak, H.S. Wong, H.K. Chai, *The potential of calcined Malaysian kaolin as a pozzolanic admixture for concrete*, **Malaysian Construction Research Journal**, **3**, 2008, pp. 21-36.
[13] A. Hussin, A.H.A. Rahman, K.Z. Ibrahim, *Mineralogy and geochemistry of clays from Malaysia and its industrial application*, **IOP Conference Series: Earth and Environmental Science**, **212**, 2018, pp. 012040.
[14] A. Tironi, M.A. Trezza, A.N. Scian, E.F. Irassar, *Kaolinitic calcined clays: factors affecting its performance as pozzolans*, **Construction and Building Materials**, **28**, 2012, pp. 276-281.
[15] B. Lothenbach, K. Scrivener, R.D. Hooton, *Supplementary cementitious materials*, **Cement and Concrete Research**, **41**, 2011, pp. 1244-1256.
[16] T.T. Haw, F. Hart, A. Rashidi, P. Pasbakhsh, *Sustainable cementitious composites reinforced with metakaolin and halloysite nanotubes for construction and building applications*, **Applied Clay Science**, **188**, 2020, pp. 105533.
[17] M.C. Juenger, R. Siddique, *Recent advances in understanding the role of supplementary cementitious materials in concrete*, **Cement and Concrete Research**, **78**, 2015, pp. 71-80.
[18] D.D.B. Nergis, P. Vizureanu, I. Ardelean, A.V. Sandu, O.C. Corbu, E. Matei, *Revealing the Influence of Microparticles on Geopolymers' Synthesis and Porosity*, **Materials**, 13(14), 2020, 3211, DOI: 10.3390/ma13143211.
[19] D.D. Burduhos Nergis, M.M.A.B. Abdullah, A.V. Sandu, P. Vizureanu, *XRD and TG-DTA Study of New Alkali Activated Materials Based on Fly Ash with Sand and Glass Powder*, **Materials**, 13, 2020, 343; doi:10.3390/ma13020343.
[20] C. He, E. Makovicky, B. Osbaeck, *Thermal stability and pozzolanic activity of calcined kaolin*, **Applied Clay Science**, **9**, 1994, pp.165-187.
[21] M. Arikan, K. Sobolev, T. Ertün, A. Yeğinobali, P. Turker, *Properties of blended cements with thermally activated kaolin*, **Construction and Building Materials**, **23**, 2009, pp. 62-70.
[22] S. Chandrasekhar, S. Ramaswamy, *Influence of mineral impurities on the properties of kaolin and its thermally treated products*, **Applied Clay Science**, **21**, 2002, pp. 133-142.
[23] M. Thommes, K. Kaneko, A.V. Neimark, J.P. Olivier, F. Rodriguez-Reinoso, J. Rouquerol, K. S. Sing, *Physisorption of gases, with special reference to the evaluation of surface area and pore size distribution (IUPAC Technical Report)*, **Pure and Applied Chemistry**, **87**, 2015, pp. 1051-1069.
[24] B. Fabbri, S. Gualtieri, C. Leonardi, *Modifications induced by the thermal treatment of kaolin and determination of reactivity of metakaolin*, **Applied Clay Science**, **73**, 2013, pp. 2-10.
[25] Y. Huang, J. Deng, W. Wang, Q. Feng, Z. Xu, *Preliminary investigation of pozzolanic properties of calcined waste kaolin*, **Materials Science**, **24**, 2018, pp. 177-184.
[26] L. T. Drzal, J. P. Rynd, T. Fort Jr, *Effects of calcination on the surface properties of kaolinite*, **Journal of Colloid and Interface Science**, **93**, 1983, pp. 126-139.
[27] D. Eberl, J. Hower, *Kaolinite synthesis: the role of the Si/Al and (alkali)/(H+) ratio in hydrothermal systems*, **Clays and Clay Minerals**, **23**, 1975, pp. 301-309.
[28] P. He, M. Wang, S. Fu, D. Jia, S. Yan, J. Yuan, J. Xu, P. Wang, Y. Zhou, *Effects of Si/Al ratio on the structure and properties of metakaolin based geopolymer*, **Ceramics International**, **42**, 2016, pp.14416-14422.
[29] R. Prost, A. Dameme, E. Huard, J. Driard, J.P. Leydecker, *Infrared study of structural OH in kaolinite, dickite, nacrite, and poorly crystalline kaolinite at 5 to 600 K*, **Clays and Clay Minerals**, **37**, 1989, pp. 464-468.
[31] R. Duarte-Silva, M.A. Villa-García, M. Rendueles, M. Díaz, *Structural, textural and protein adsorption properties of kaolinite and surface modified kaolinite adsorbents*, **Applied Clay Science**, **90**, 2014, pp.73-80.

[31] L. Edomwonyi-Otu, B.O. Aderemi, A.S. Ahmed, N.J. Coville, M. Maaza, *Influence of thermal treatment on kankara kaolinite*, **Opticon1826**, **15**, 2013, pp. 1-5.
[32] J. Madejová, *FTIR techniques in clay mineral studies*, **Vibrational spectroscopy**, **31**, 2003, pp. 1-10.
[33] T. Danner, G. Norden, H. Justnes, *Characterisation of calcined raw clays suitable as supplementary cementitious materials*, **Applied Clay Science**, **162**, 2018, pp. 391-402.

Received: November 5, 2020
Accepted: August 20, 2021